CRNOGORSKA AKADEMIJA NAUKA I UMJETNOSTI
GLASNIK ODJELJENJA PRIRODNIH NAUKA, 27, 2024.

ČERNOGORSKAYA AKADEMIYA NAUK I ISSKUSTV
GLASNIK OTDELENIYA ESTESTVENNYH NAUK, 27, 2024.

THE MONTENEGRIN ACADEMY OF SCIENCES AND ARTS
PROCEEDINGS OF THE SECTION OF NATURAL SCIENCES, 27, 2024

UDK 539.319

*Marko V. Lubarda, Vlado A. Lubarda**

Deriving the force-displacement relationships for indentation problems without solving the corresponding boundary-value problems

A b s t r a c t

The force-displacement relationships for spherical, cylindrical and conical indentations, and indentations by a flat cylindrical or rectangular punch are derived up to a single constant by dimensional analysis and basic geometric and mechanics considerations, without solving the corresponding boundary-value problems. Only one experimental data point suffices to fully determine the force-displacement relationship of elastic indentation, without knowing the pressure distribution in the contact region. Results obtained by using exact or proposed trial pressure distributions are compared and discussed.

Keywords: conical indenter; contact mechanics; cylindrical indenter; dimensional analysis; elasticity; indentation; pressure; rectangular punch; spherical indenter

1 Introduction

Indentation testing is of great importance for the determination of the hardness of a material [1]-[4]. Indenter is pressed into the material to produce a small impression and the mechanical properties are estimated from the relationship between the applied force and the depth of the indentation. Various types of indenters are in use, as described in standard textbooks of materials science and engineering [5, 6]. The Brinell hardness involves spherical ball indenters, while the Rockwell hardness is based on conical indenters. In this paper we revisit the derivation of the relationship between the applied force and the depth of the indentation in the range of infinitesimal elastic deformation. Spherical, cylindrical, and conical indenters, pressed into an isotropic elastic half-space, are analyzed, as well

*M.V. Lubarda, Department of Mechanical and Aerospace Engineering, University of California, San Diego; Member of the Center for Young Scientists and Artists, Montenegrin Academy of Sciences and Arts.
V.A. Lubarda, NanoEngineering Department, University of California, San Diego; Member of the Montenegrin Academy of Sciences and Arts.

as indenters in the form of flat cylindrical or rectangular punches [7]-[11]. It is shown that in each of these cases the force-displacement relationship can be derived up to a single dimensionless constant by dimensional analysis and by basic geometric and mechanics considerations, without solving the entire indentation boundary value problem at hand. The mechanics considerations include only the referral to fundamental Boussinesq or Flamant problems of a concentrated vertical force on the surface of a half-space [16, 7], and the energy requirement that the work of the indentation force must be equal to the work of statically equivalent pressure transmitted to the half-space by the indenter on the corresponding displacements below the indenter. To specify the unknown constant, the expression for the pressure distribution within the contact zone needs to be reasonably assumed. If this is the correct pressure distribution, e.g., a semi-ellipsoidal (semi-elliptical) in the case of spherical (cylindrical) indentation, the exact value of the constant is obtained, but using any reasonable trial pressure distribution, including a uniform pressure distribution in the case of indentation by a spherical ball, gives an error of less than 5%. The results obtained for different approximate pressure distributions are discussed. The indentation stiffness is evaluated for all considered types of indentation. Because for each considered indenter only one parameter in the force-displacement relationship is not specified by the presented analysis exactly, only one experimental data point is needed to fully specify the force-indentation relationship, without making any assumption about the contact pressure.

2 Indentation by a rigid spherical ball

Figure 1 shows the cross section of a smooth rigid spherical ball of radius R pressed against an isotropic elastic half-space with elastic constants E and ν. The depth of the indentation due to applied force F is denoted by δ. The ball is in contact with the material of a half-space for $w(a) \leq z \leq w(0)$, where $w(0) = \delta$ and $w(a) = \delta - \delta_0$, where δ_0 is the height of the contact zone. The vertical displacement $w = w(r)$ within the contact zone corresponds to spherical shape of the indenter, thus satisfying the equation $r^2 + [w(r) + R - \delta]^2 = R^2$. For shallow indentation, $w(r) \ll R$, this spherical shape can be approximated by the paraboloid shape

$$w(r) = \delta - \frac{r^2}{2R}\,, \quad r \leq a\,, \tag{2.1}$$

where a is the radius of the base of the contact region (radius of the projected contact surface), as sketched in Fig. 1. The height of the spherical sector of the ball which is in contact with a half-space is $\delta_0 = a^2/(2R)$, because a is the geometric mean of δ_0 and $2R - \delta_0$, with $\delta_0 \ll R$. The objective is to determine the force-displacement relationship $F = F(\delta)$.

2.1 Dimensional analysis

It is reasonable to assume that the relationship between F and δ involves the dimensional quantities E and a. The radius of the ball R is not explicitly included because it is expected, on physical and geometric grounds, that a unique value of R corresponds to given values of a and δ. Furthermore, by self-similarity of the elastic spherical indentation process, the height of the contact zone δ_0 is expected to be proportional to the indentation depth δ, independently of the value of F, and does not need to be included explicitly either. Therefore, by applying the Buckingham Π theorem [12, 13]

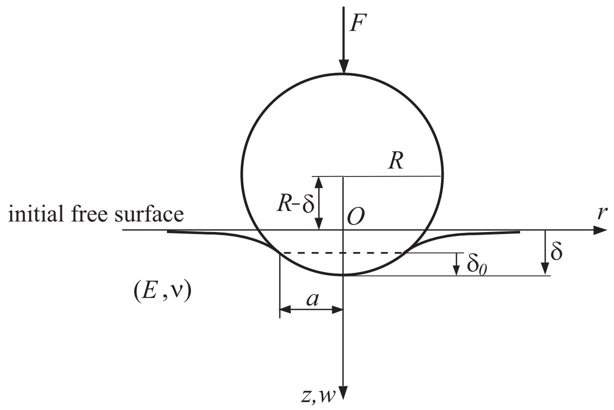

Figure 1: A rigid spherical ball of radius R pressed into an elastic half-space by the force F. The depth of the indentation is δ, and a is the radius of the contact at $z = \delta - \delta_0$, where δ_0 is the height of the contact zone. The elastic properties of a half-space are E and ν.

one can readily identify the following two independent non-dimensional groups

$$\Pi_1 = \frac{\delta}{a}, \quad \Pi_2 = \frac{F}{Ea^2}, \tag{2.2}$$

and they must be related through some function f by

$$\frac{\delta}{a} = f\left(\frac{F}{Ea^2}\right). \tag{2.3}$$

In linear elasticity, for a given pressure distribution acting on the surface of a half-space over a circular region of a given radius a, statically equivalent to given force F, the displacement δ must depend linearly on F/E, thus (2.3) simplifies to

$$\frac{\delta}{a} = c(\nu)\,\frac{F}{Ea^2} \quad \Rightarrow \quad \delta = c(\nu)\,\frac{F}{Ea}, \tag{2.4}$$

where $c(\nu)$ is the Poisson ratio dependent coefficient, to be determined in the sequel. An alternative dimensional analysis of contact problems was used in [7], p. 89-90; see also [14, 15]. Note that a in (2.4) also depends on F, thus (2.4) is a nonlinear relationship between the indentation depth δ and the force F.

2.2 The coefficient c(ν)

We show next, without solving the complete indentation boundary-value problem, that $c(\nu) = c_0(1-\nu^2)$, where $c_0 = \text{const}$. This is accomplished by referring to the fundamental Boussinesq problem of a concentrated vertical force acting on the surface of a half-space (Fig. 2a). The vertical component of the displacement of the point of the free surface $z = 0$, at a distance r from the point of the application of F is (e.g., [7], (3.22b), p. 52, or [16], eq. (205), p. 365)

$$w(r) = \frac{1-\nu^2}{E}\,\frac{F}{\pi r}. \tag{2.5}$$

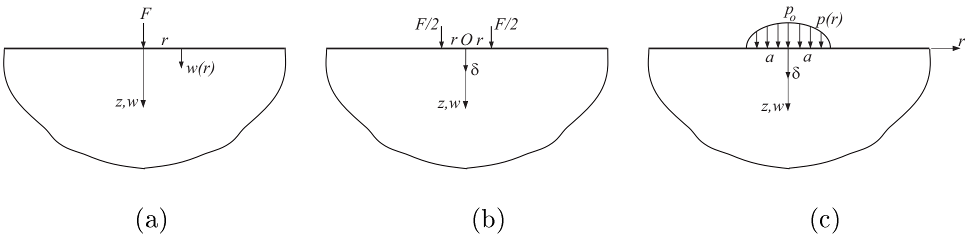

Figure 2: (a) A vertical concentrated force F applied to the surface of a half-space. The vertical component of the displacement at the surface point at a distance r from the force is $w(r)$. (b) The displacement of the midpoint O between two vertical forces $F/2$ at the distance $2r$ from each other is denoted by δ. (c) The axisymmetric pressure distribution $p = p(r)$ applied to the surface of a half-space within the circle $r \leq a$, with $p(0) = p_0$ and $p(a) = 0$.

If there are two vertical forces, each of magnitude $F/2$, acting on the surface of a half-space at a distance $2r$ from each other (Fig. 2b), the vertical displacement of the midpoint O is, by superposition using (2.5),

$$\delta = \frac{1-\nu^2}{E}\,\frac{F}{\pi r}\,. \tag{2.6}$$

The same vertical displacement is produced at the center of the circle of radius r by uniformly distributed line force of magnitude $F/(2\pi r)$ (per unit length), acting along that circle. Thus it follows by integration that the vertical displacement at the center of a circular region of radius a, loaded by an arbitrary axisymmetric pressure distribution $p = p(r)$, Fig. 2c, is

$$\delta = \frac{1-\nu^2}{E}\int_0^a \frac{p(r)2\pi r\mathrm{d}r}{\pi r} \equiv 2\,\frac{1-\nu^2}{E}\int_0^a p(r)\mathrm{d}r\,. \tag{2.7}$$

By symmetry, the slope of the vertical line (z-axis) is equal to zero.

Because in the indentation by a spherical ball the pressure over the contact region $r \leq a$ is axisymmetric, and $F = \int_0^a p(r)2\pi r\mathrm{d}r$, the comparison of (2.4) and (2.7) shows that

$$c(\nu) = c_0(1-\nu^2)\,, \quad c_0 = \frac{1}{\pi}\,\frac{\int_0^1 p(\rho)\mathrm{d}\rho}{\int_0^1 \rho p(\rho)\mathrm{d}\rho}\,, \quad \rho = \frac{r}{a}\,. \tag{2.8}$$

Consequently, (2.4) becomes

$$\delta = c_0\,\frac{1-\nu^2}{E}\,\frac{F}{a}\,, \quad \text{or} \quad F = \frac{1}{c_0}\,\frac{E}{1-\nu^2}\,a\delta\,. \tag{2.9}$$

Because F in this expression depends on the product of a and δ, and a depends on δ, equation (2.9) implies a nonlinear force-displacement relation. Also, the average pressure $\bar{p} = F/\pi a^2$ is proportional to δ/a.

2.3 Expression for a in terms of R and δ

The relationship between the height of the contact zone δ_0, the contact radius a, and the radius of the ball R has already been established by spherical geometry of the indenter and is given in linear theory by $a^2 = 2R\delta_0$. One cannot identify the corresponding relationship among a, R, and δ, without solving the entire boundary-value problem, but one can observe by self-similarity of spherical indentation process within the elastic range of indentation that δ and δ_0 should be proportional to each other, $\delta_0 = k\delta$, and, therefore,

$$a^2 = 2kR\delta\,, \quad k = \text{const.} \tag{2.10}$$

If (2.10) is substituted into (2.9), it follows that

$$F = \zeta\, \frac{E}{1-\nu^2}\, R^{1/2}\, \delta^{3/2}\,, \quad \zeta = \frac{\sqrt{2k}}{c_0}\,, \tag{2.11}$$

which establishes the well-known $F \sim \delta^{3/2}$ force-indentation relationship of spherical indentation. It remains to determine or estimate the values of non-dimensional constants c_0 and k, and thus ζ. From an experimental point of view, only one experimental data point would, in principle, suffice to specify ζ and thus, from (2.11), the force-displacement relationship. If multiple measurements of F versus δ are made, ζ can be determined with reduced uncertainty from the slope of the best linear fit of F versus $\delta^{3/2}$ data. We proceed with analytical estimates of c_0 and k.

2.4 Determination of c_0 and k

The constants c_0 and k cannot be determined exactly without solving the entire boundary-value problem of spherical indentation. However, if one assumes that the pressure distribution within the contact region $r \leq a$ is ellipsoidal

$$p(r) = p_0 \left(1 - \frac{r^2}{a^2}\right)^{1/2}\,, \quad p_0 = \frac{3}{2}\,\bar{p}\,, \quad \bar{p} = \frac{F}{\pi a^2}\,, \tag{2.12}$$

it readily follows from (2.8) that

$$c_0 = \frac{3}{4}\,. \tag{2.13}$$

Of course, the semi-ellipsoidal pressure distribution is known to be the correct pressure distribution (Hertz pressure) from the existing solution to the boundary-value problem of indentation by a spherical ball, e.g., [7], p. 92 and [10], p. 87, but it could have been reasonably assumed even without referring to that solution, because $p(r)$ in (2.12) has a maximum value at the center, with the zero slope, and it vanishes along the edge of the contact $r = a$ (to avoid stress discontinuity across the edge), with an infinite pressure gradient in the radial direction (to enhance the indentation), all of which features could have been reasonably anticipated. An alternative pressure distribution with such features is $p(r) \sim \cos^{1/2}(\pi r/2a)$; by (2.8) this would give $c_0 = 0.7635$, which is only 1.8% different from the exact value $c_0 = 0.75$, corresponding to semi-ellipsoidal pressure distribution.

It remains to determine the constant k. To that goal, we rewrite (2.1) by using (2.10) as

$$w(r) = \delta \left(1 - k\,\frac{r^2}{a^2}\right)\,, \tag{2.14}$$

and impose the condition that the work done by the force F on the displacement δ,

$$W_F = \int_0^\delta F(\delta)\mathrm{d}\delta = \frac{2}{5}\,F\delta\,, \tag{2.15}$$

must be equal to the work done by the statically equivalent pressure distribution $p(r)$ on the displacement $w(r)$,

$$W_p = \frac{1}{2}\int_0^a p(r)w(r)2\pi r\mathrm{d}r\,. \tag{2.16}$$

Upon substitution of (2.12) and (2.14) into (2.16), it follows that

$$W_p = \frac{1}{2}\,F\delta\left(1-\frac{2k}{5}\right). \tag{2.17}$$

Thus, by equating (2.15) and (2.17), one obtains $k = 1/2$, i.e.,

$$\delta_0 = \frac{\delta}{2}\,,\quad a^2 = R\delta\,. \tag{2.18}$$

The energy considerations in the analysis of elastic contact, with different objectives, have also been used in [17].

The substitution of $c_0 = 3/4$ and $k = 1/2$ into (2.11) gives $\zeta = 3/4$ and thus the famous nonlinear relationship of spherical indentation (e.g., [7], eq. (4.23), p. 93; [18], eq. (11.50), p. 364),

$$F = \frac{4}{3}\,\frac{E}{1-\nu^2}\,R^{1/2}\,\delta^{3/2}\,. \tag{2.19}$$

Consequently, for a given indentation depth δ, the larger R the larger F. On the other hand, for a given contact radius a, the larger R the smaller F, because $\delta = a^2/R$.

The total strain energy stored in the half-space is $U = 2F\delta/5 = (8E_*/15)R^{1/2}\delta^{5/2}$, where $E_* = E/(1-\nu^2)$, such that $F = \partial U/\partial\delta$; e.g., [19]. The elastic indentation stiffness is $K = \partial^2 U/\partial\delta^2 = \partial F/\partial\delta = 2E_*R^{1/2}\delta^{1/2}$. Furthermore, the average pressure in the contact region is proportional to a/R (or δ/a),

$$\bar{p} = \frac{F}{\pi a^2} = \frac{4}{3\pi}\,\frac{E}{1-\nu^2}\,\frac{a}{R}\,. \tag{2.20}$$

In the analysis of the indentation problems beyond elastic range, it is often assumed that the average pressure is $\kappa(a/R)^{1/n}$, where κ and $n(>1)$ are material parameters (Meyer's law [20, 21]), generalizing the linear relationship (2.20).

2.5 Trial pressure distributions

If an arbitrary trial pressure distribution is assumed, it readily follows that the constant k is determined from

$$k = \frac{1}{5}\,\frac{\int_0^1 \rho p(\rho)\mathrm{d}\rho}{\int_0^1 \rho^3 p(\rho)\mathrm{d}\rho}\,. \tag{2.21}$$

For example, if $p(\rho) \sim \bar{p}\cos^{1/2}(\pi\rho/2)$, then $k = 0.5105$, and since in this case $c_0 = 0.7635$, one obtains in eq. (2.19) $\zeta = 1.3233$ rather than $4/3$, which is an error of only 0.75%. If a uniform pressure distribution ($p = \bar{p} = F/\pi a^2$) is assumed, then $k = 0.4$, $c_0 = 0.6366$, and $\zeta = 1.405$, which is an error of about 5%. If $p(\rho) \sim \bar{p}(1-\rho^2)^{1/3}$ is used, then $k = 0.4667$, $c_0 = 0.7141$, and $\zeta = 1.3628$, the error being less than 1.5%. Finally, if $p(\rho) \sim \bar{p}(1-\rho^2)^{2/3}$, then $k = 0.5333$, $c_0 = 0.7843$, and $\zeta = 1.3169$, with an error of less than 1.25%. The proposed trial pressure distributions are shown graphically in Fig. 3a, all being normalized by the average pressure $\bar{p} = F/\pi a^2$.

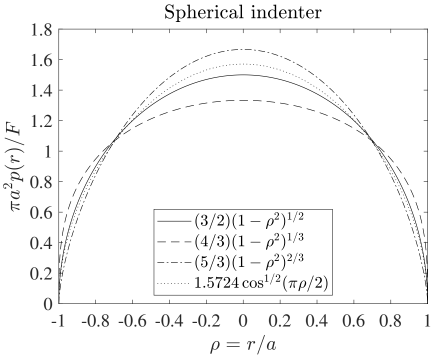

(a)

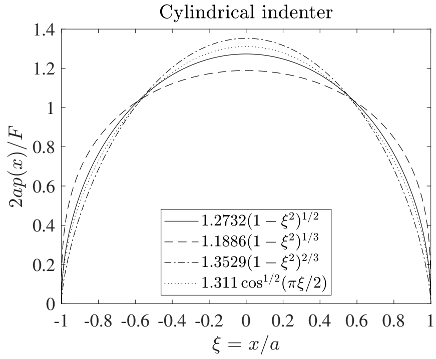

(b)

Figure 3: (a) The shapes of four considered pressure distributions, normalized by the average pressure $\bar{p} = F/\pi a^2$, in the case of the indentation by a spherical ball. (b) The shapes of four considered pressure distributions, normalized by $F/2a$, in the case of the indentation by a circular cylinder. The coefficient $1.2732 = 4/\pi$; the other shown coefficients are obtained numerically, so that the force F is the same in each case. For example, $1.311 = \pi/4E(\pi/4, 2)$, where $E(\pi/4, 2)$ is the value of the incomplete elliptic integral of the second kind at $\pi/4$.

3 Indentation by a rigid circular cylinder

The cross section of an infinitely long smooth rigid cylindrical indenter of radius R pressed against an isotropic elastic half-space is shown in Fig. 4a. The applied force per unit length of the cylinder is F, and the depth of the resulting indentation relative to the initial level of the free surface (shown dashed) is δ. The height of the contact with the material of a half-space is δ_0, and $2a$ is the maximum width of the contact. For shallow indentation, the circular contact can be approximated by the parabolic shape

$$w(x) = \delta - \delta_0 \, \frac{x^2}{a^2} \, , \quad |x| \leq a \, , \tag{3.1}$$

where $w(0) = \delta$ and $w(\pm a) = \delta - \delta_0$. The rigid-body translation is eliminated by requiring that $w(\pm b) = 0$, for a selected value of b. By circular geometry, a is the geometric mean of $2R - \delta_0$ and δ_0, which for $\delta_0 \ll R$ simplifies to $a^2 = 2R\delta_0$, independently of b.

3.1 Dimensional analysis

The relationship between F and δ_0 is expected to involve the plane-strain modulus of elasticity $E_* = E/(1-\nu^2)$ and the contact semi-width a. The radius of the cylinder does not need to be explicitly included because it depends on a and δ_0, being related to them by $a^2 = 2R\delta_0$. By applying the Π theorem the following two independent non-dimensional groups can then be identified

$$\Pi_1 = \frac{\delta_0}{a} \, , \quad \Pi_2 = \frac{F}{E_* a} \, , \tag{3.2}$$

which must be related by

$$\frac{\delta_0}{a} = f\left(\frac{F}{E_* a}\right). \tag{3.3}$$

For a given pressure distribution due to a given force F, acting over a given length $2a$ of the surface of a half-space, the displacement δ_0 in plain-strain linear elasticity must depend linearly on F/E_*, and (3.3) reduces to

$$\frac{\delta_0}{a} = c_0\,\frac{F}{E_* a} \quad \Rightarrow \quad \delta_0 = c_0\,\frac{F}{E_*}\,, \quad c_0 = \text{const.} \tag{3.4}$$

Thus, for a given indentation force F, the contact height is proportional to F/E_*, independently

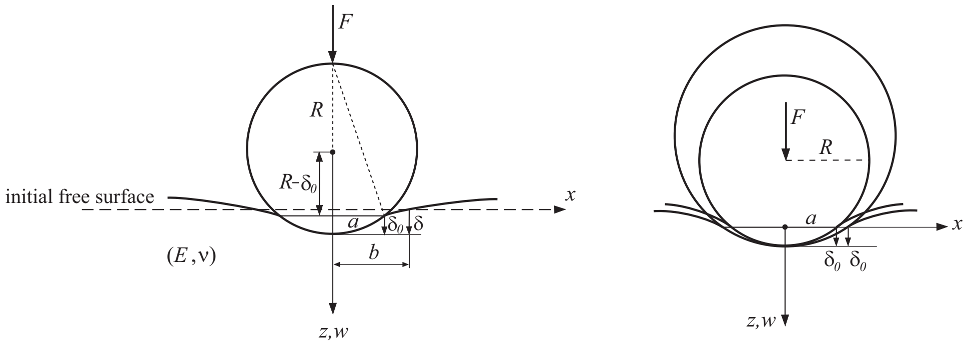

(a) (b)

Figure 4: (a) A rigid circular cylinder of radius R pressed into an elastic half-space by a force F (per unit length of the cylinder). The height of the cylindrical cap in contact with the material of a half-space is δ_0, and $2a$ is the corresponding width of the contact. The depth of the indentation relative to the initial level of the free surface (shown dashed) is δ. The elastic properties of a half-space are E and ν. (b) A given indentation force F produces the same contact height δ_0, independently of the radius of the cylinder R and the width of the contact zone $2a$. The contact height $\delta_0 \sim F$, while $a \sim F^{1/2}$, such that $a^2 = 2R\delta_0$.

of a and R (Fig. 4b). The contact semi-width a is proportional to $F^{1/2}$, because $a^2 = 2R\delta_0 = 2c_0FR/E_*$. In summary, in contrast to spherical indentation, the $F = F(\delta_0)$ relationship of cylindrical indentation is linear and given by

$$F = \frac{1}{c_0}\,\frac{E}{1-\nu^2}\,\delta_0\,. \tag{3.5}$$

3.2 Estimate of c_0

We elaborate next on the determination of c_0, without solving the complete boundary-value problem, by referring only to Flamant's problem of a concentrated vertical line force acting on the free surface of a half-space (Fig. 5a). The vertical component of the displacement of the point of the free surface $z = 0$, at a distance x from the point of the application of F, is (e.g., equation following (2.19b), p.

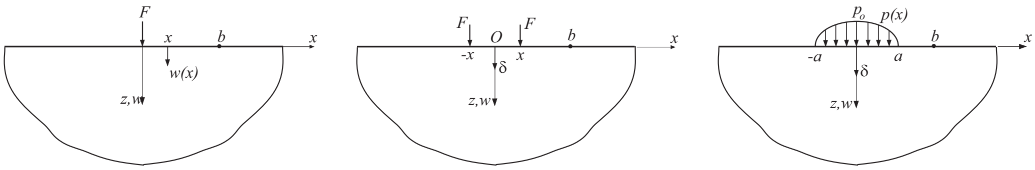

(a) (b) (c)

Figure 5: (a) A concentrated line force F (per unit length) applied to the surface of a half-space. The vertical component of the displacement at the surface point at a distance x from the force is $w(x)$. The vertical displacement $w(b) = 0$, at the selected point $x = b$. (b) The displacement of the midpoint O between two vertical line forces F at a distance $2x$ from each other is denoted by δ. (c) The symmetric pressure distribution $p = p(x)$ applied on the surface of a half-space within the range $|x| \leq a$, with $p(0) = p_0$ and $p(\pm a) = 0$. The vertical displacement at $x = 0$ is denoted by δ.

17, of [7])

$$w(x) = \frac{2F}{\pi} \frac{1-\nu^2}{E} \ln \frac{b}{x}, \tag{3.6}$$

where the vertical rigid-body displacement is specified by requiring that $w(\pm b) = 0$ for a selected value of b. If there are two concentrated line forces at the positions $\pm x$ (Fig. 5b), the vertical displacement at the point midway between them is, by superposition,

$$\delta_0 = \frac{2F}{\pi} \frac{1-\nu^2}{E} \left(\ln \frac{b-x}{x} + \ln \frac{b+x}{x} \right) \equiv \frac{2F}{\pi} \frac{1-\nu^2}{E} \ln \left(\frac{b^2}{x^2} - 1 \right). \tag{3.7}$$

The vertical displacement at the center of a symmetric pressure distribution $p = p(x)$ (per unit length of the cylinder, Fig. 5c) is obtained from (3.7) by integration,

$$\delta = \frac{2}{\pi} \frac{1-\nu^2}{E} \int_0^a p(x) \ln \left(\frac{b^2}{x^2} - 1 \right) \mathrm{d}x. \tag{3.8}$$

If $b = a$, (3.8) gives

$$\delta_0 = \frac{2}{\pi} \frac{1-\nu^2}{E} \int_0^a p(x) \ln \left(\frac{a^2}{x^2} - 1 \right) \mathrm{d}x. \tag{3.9}$$

The comparison of (3.4) and (3.9) establishes that

$$c_0 = \frac{1}{\pi} \frac{\int_0^a p(x) \ln(a^2/x^2 - 1)\mathrm{d}x}{\int_0^a p(x)\mathrm{d}x}. \tag{3.10}$$

If $p(x)$ is assumed to be semi-elliptical in shape ([7], eq. (4.44), p. 101; [10], eq. (5.4.3a), p. 92; [11], eq. (2.29), p. 55) ,

$$p(x) = p_0 \left(1 - \frac{x^2}{a^2} \right)^{1/2}, \quad p_0 = \frac{4}{\pi}\,\bar{p} = \frac{2F}{\pi a}, \quad \bar{p} = \frac{F}{2a}, \tag{3.11}$$

it follows that

$$\int_0^a p(x)\,\ln\left(\frac{a^2}{x^2}-1\right)\mathrm{d}x = \frac{\pi}{2}\,p_0 a\,, \qquad \int_0^a p(x)\mathrm{d}x = \frac{\pi}{4}\,p_0 a\,, \tag{3.12}$$

and, therefore, from (3.10),

$$c_0 = \frac{2}{\pi}\,. \tag{3.13}$$

Consequently, (3.5) becomes

$$F = \frac{\pi}{2}\,\frac{E}{1-\nu^2}\,\delta_0\,. \tag{3.14}$$

Since $a^2 = 2R\delta_0$, (3.14) implies that a is proportional to $F^{1/2}$, independently of b, i.e.,

$$a = \left[\frac{4(1-\nu^2)R}{\pi E}\right]^{1/2} F^{1/2}\,. \tag{3.15}$$

Furthermore, the average pressure in the contact region is proportional to a/R, similarly to the case of the indentation by a spherical ball, see (2.20), i.e.,

$$\bar{p} = \frac{F}{2a} = \frac{\pi}{8}\,\frac{E}{1-\nu^2}\,\frac{a}{R}\,. \tag{3.16}$$

The expression (3.14) is the exact expression for F in terms of δ_0, because the assumed pressure distribution (3.11) is the actual pressure distribution of the indentation by a circular cylinder (as can be deduced from eq. (2.48), page 32 of [7], in the case $n=1$ of their analysis). However, even if one used a reasonable approximate pressure distribution, a reasonably accurate value of c_0 would have been obtained. For example, if the pressure distribution is assumed to be $p(x) \sim \bar{p}(1-x^2/a^2)^{1/3}$, it follows that $c_0 = 1.8315/\pi$, with an error of 8.4%, while $p(x) =\sim \bar{p}(1-x^2/a^2)^{2/3}$ gives $c_0 = 2.1453/\pi$, the error being 7.3%. On the other hand, if it is assumed that $p(x) \sim \bar{p}\cos^{1/2}(\pi x/2a)$, the coefficient $c_0 = 2.0591/\pi$, which is less than 3% different from the exact value $c_0 = 2/\pi$. The utilized pressure distributions are shown graphically in Fig. 3b, all being normalized by the average pressure $\bar{p} = F/2a$.

3.3 Determination of the indentation depth δ

By substituting the expression for the pressure distribution (3.11) into (3.8), and by using (3.14) to express F in terms of δ_0, the indentation depth becomes

$$\delta = \frac{2\delta_0}{a}\int_0^a (1-x^2/a^2)^{1/2}\,\ln(b^2/x^2-1)\,\mathrm{d}x\,. \tag{3.17}$$

i.e., upon integration,

$$\frac{\delta}{\delta_0} = \left(\frac{b}{a}\right)^2 - \frac{b}{a}\sqrt{\left(\frac{b}{a}\right)^2-1} + \ln\left[\frac{b}{a}+\sqrt{\left(\frac{b}{a}\right)^2-1}\right]\,. \tag{3.18}$$

The nonlinear relationship between δ and F can be readily recognized from (3.18) by observing that

$$\delta_0 = \frac{R}{2}\,\frac{F}{F_*}\,, \quad a = R\left(\frac{F}{F_*}\right)^{1/2}\,, \quad F_* = \frac{\pi}{4}\,E_* R\,, \quad E_* = \frac{E}{1-\nu^2}\,. \tag{3.19}$$

When this is substituted into (3.18), we obtain the nonlinear force-indentation relationship

$$\delta = \frac{R}{2}\left\{\left(\frac{b}{R}\right)^2 - \frac{b}{R}\sqrt{\left(\frac{b}{R}\right)^2 - \frac{F}{F_*}} + f\ln\left[\frac{b}{R} + \sqrt{\left(\frac{b}{R}\right)^2 - \frac{F}{F_*}}\right] - \frac{1}{2}\frac{F}{F_*}\ln\frac{F}{F_*}\right\}. \tag{3.20}$$

For $b \gg a$, (3.20) simplifies to

$$\delta = \frac{R}{4}\frac{F}{F_*}\left(1 - \ln\frac{F}{F_*} + 2\ln\frac{2b}{R}\right). \tag{3.21}$$

The corresponding elastic compliance is

$$K^{-1} = \frac{\mathrm{d}\delta}{\mathrm{d}F} = \frac{1}{\pi E_*}\left(2\ln\frac{2b}{R} - \ln\frac{F}{F_*}\right). \tag{3.22}$$

The plot of normalized $F/F_{\max}$ vs. δ/R, where $F_{\max} = 10^{-3}F_*$ (good for metals before the onset

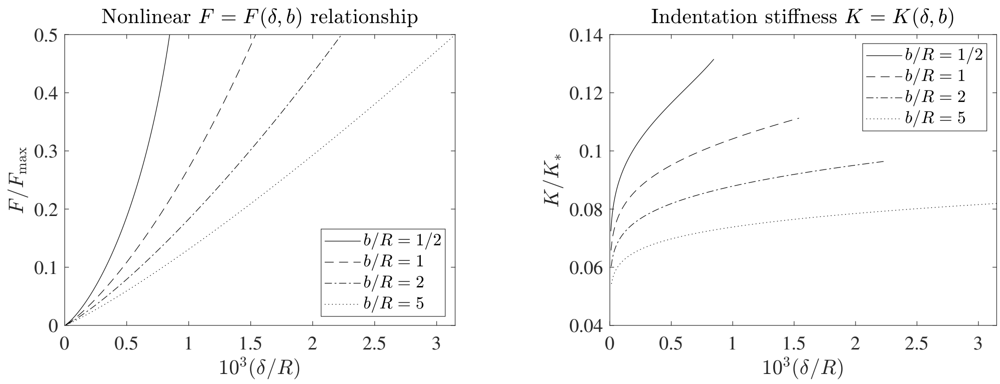

(a) (b)

Figure 6: (a) The normalized indentation force $F/F_{\max}$ vs. the normalized indentation depth of cylindrical indentation for the four shown values of b/R. The normalizing force is $F_{\max} = 10^{-3}F_*$, where $F_* = (\pi/4)E_*R$. (b) The corresponding normalized indentation stiffness K/K_* vs. the normalized indentation depth $10^3(\delta/R)$, where R is the radius of the cylindrical indenter and $K_* = \pi E_*$.

of plastic yield), is shown in Fig. 6a, and the plot of the corresponding normalized indentation stiffness K/K_* vs. δ/R, where $K_* = \pi E_*$ is shown in Fig. 6b. The four curves correspond to four selected values of the ratio b/R. As expected, the smaller the value of b the greater the stiffness K, for any value of δ. In each case, the stiffness is equal to zero at $\delta = 0$. Recall that the initial indentation stiffness for spherical indentation ($K \sim \delta^{1/2}$) is also equal to zero.

It is pointed out that there exist a minimum value of b for which the cylindrical indentation is geometrically and physically possible. This follows from the work condition $W_F = W_p$, which turns out to be satisfied for $b \geq b_{\min}$, as recently elaborated upon and discussed in [22]. For applications, e.g., in an approximate analysis of cylindrical indentation of a large but finite elastic block [9], large values of $b \gg a$ are most useful. The effects of the finite length of the cylindrical indenter were considered in [23, 24]. Cylindrical indentation of an elastic layer bonded to a rigid substrate has been analyzed in [25]-[27]. The studies of cylindrical indentation of an elastic half-space with or without surface tension effects [28]-[30], and cylindrical indentation of functionally graded half-space [31, 32] have also been performed. Micropolar elasticity effects have been considered in [33]. In an approximate analysis of indentation by a circular cylinder of a thin elastic layer (of thickness h) placed on a frictionless rigid substrate [7], it was assumed that the stress state outside the contact region $|x| \geq a$ is identically equal to zero, while $\sigma_x = 0$, $\sigma_z(x) = E_*\epsilon_z(x)$, and $\sigma_y(x) = \nu\sigma_z(x)$ (plain strain), where $\epsilon_z(x) = -w(x)/h$ and $w(x) = \delta(1 - x^2/a^2)$. This yields the pressure distribution $p(x) \sim (1 - x^2/a^2)$ and the force-indentation relationship $F \sim E_*(\sqrt{R}/h)\delta^{3/2}$. If the layer is bonded to the substrate, a modified approximate analysis for an incompressible layer [7] yields $p(x) \sim (1 - x^2/a^2)^2$ and the force-indentation relationship $F \sim E(\sqrt{R}/h)^3\delta^{5/2}$. See also references [26, 27].

4 Indentation by a flat cylindrical punch

Figure 7a shows a smooth flat circular cylindrical punch of radius R indented into an isotropic elastic half-space with elastic constants E and ν. The depth of the indentation due to the applied force F is δ. Because the contact is in this case a circle of known radius $a = R$, the force F for linear elastic indentation is proportional to the depth of indentation δ. Thus, by dimensional analysis it immediately follows that $F = cE_*R\delta$, where c is a constant. This linearity also follows from eq. (2.7), i.e.,

$$\delta = \frac{2}{E_*}\int_0^R p(r)\mathrm{d}r\,, \tag{4.1}$$

and the expression for the force in terms of the contact pressure

$$F = 2\pi\int_0^R rp(r)\mathrm{d}r\,. \tag{4.2}$$

Indeed, by dividing (4.2) with (4.1), one obtains

$$\frac{F}{\delta} = \pi E_*\,\frac{\int_0^R rp(r)\mathrm{d}r}{\int_0^R p(r)\mathrm{d}r}\,. \tag{4.3}$$

Therefore,

$$F = cE_*R\delta\,, \quad c = \pi\,\frac{\int_0^1 \rho p(\rho)\mathrm{d}\rho}{\int_0^1 p(\rho)\mathrm{d}\rho}\,, \quad \rho = \frac{r}{R}\,. \tag{4.4}$$

The pressure distribution $p = p(r)$ within the contact circle is expected to have a singularity along the edge $r = R$ (where a small amount of plastic deformation is inevitable, but ignored in this analysis), and some minimum value p_0 with a zero slope at the center $r = 0$. It is thus reasonable to assume that

$$p = \frac{p_0}{\sqrt{1 - r^2/R^2}}\,, \quad p_0 = \frac{\bar{p}}{2}\,, \quad \bar{p} = \frac{F}{\pi R^2}\,. \tag{4.5}$$

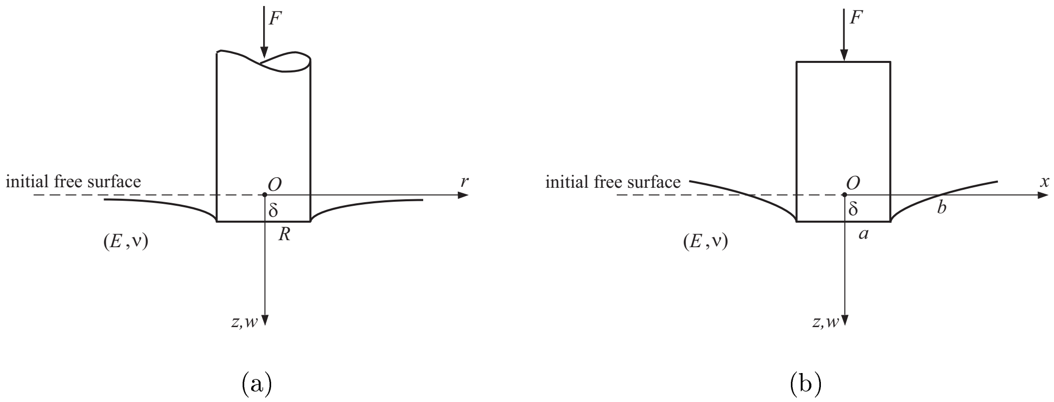

Figure 7: (a) A circular cylindrical punch with a smooth flat end of radius R indented into an isotropic elastic half-space with elastic constants E and ν. The depth of the indentation due to the applied force F is δ. There is a pressure singularity along the edge $r = R$, and an infinite displacement slope $\mathrm{d}w/\mathrm{d}r$ at $r = R^+$, embedded in the displacement profile $w(r) = (2\delta/\pi)\arcsin(R/r)$, $r \geq R^+$, predicted by linear elasticity theory. (b) A long rectangular punch of width $2a$ indented into a half-space. The displacement profile of the surface points outside the punch according to linear elasticity theory is $w(x) = \delta - (2F/\pi E_*)\ln[x/a + (x^2/a^2 - 1)^{1/2}]$, $x \geq a$, where the indentation depth δ corresponds to the imposed displacement condition $w(x = \pm b) = 0$, for an arbitrarily selected value of $b > a$.

It (4.5) is substituted into (4.4), it follows that $c = 2$, and the force-displacement relationship becomes

$$F = 2E_* R\delta\,. \tag{4.6}$$

The pressure distribution (4.5) is the actual pressure distribution below the punch, as shown in the textbooks of elasticity or contact mechanics, e.g., [10], p. 92-96, thus $c = 2$ is the exact value of c. If a trial pressure distribution $p(r) = p_0[1 - \ln(1 - r^2/R^2)]$ is used, the value of c determined from (4.4) is $c = 1.9468$, which is only 2.7% below the exact value. The simplest (uniform) trial pressure $p = \bar{p} = F/(\pi R^2)$ gives $c = 1.571$, which is 21.5% below the exact value. The strain energy stored in the half-space is $U = F\delta/2 = E_* R\delta^2$, with the corresponding constant indentation stiffness, $K = \partial^2 U/\partial\delta^2 = \partial F/\partial\delta = 2E_* R$.

4.1 Indentation by a long rectangular punch

Figure 7b shows a long smooth rectangular punch of width $2a$, indented into a half-space by a vertical line force F. The non-dimensional groups are δ/a and $F/E_* a$, and for linear elastic indentation it follows that the line force proportional to the depth of indentation δ, i.e., $F = cE_*\delta$, where c is a constant which can be defined in terms of the contact pressure as follows. Assuming that the vertical displacements of the points $x = \pm b$, where $b > a$, are equal to zero, $w(x = \pm b) = 0$, the vertical displacement along the center line of the contact is, similarly to (3.8),

$$\delta = \frac{2}{\pi E_*} \int_0^a p(x) \ln\left(\frac{b^2}{x^2} - 1\right) \mathrm{d}x\,, \quad b > a\,. \tag{4.7}$$

On the other hand,

$$F = 2 \int_0^a p(x) \mathrm{d}x\,, \tag{4.8}$$

and by dividing (4.8) with (4.7) if follows that

$$\frac{F}{\delta} = \pi E_* \frac{\int_0^a p(x)\mathrm{d}x}{\int_0^a p(x) \ln(b^2/x^2 - 1)\mathrm{d}x}\,. \tag{4.9}$$

Consequently,

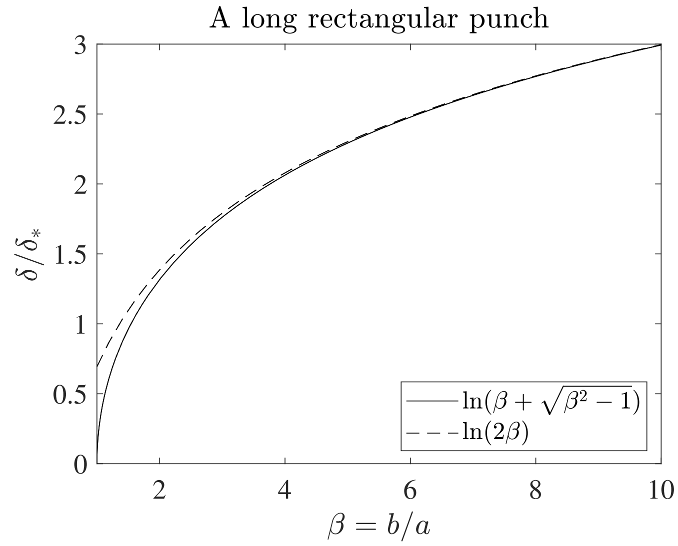

Figure 8: The normalized depth of indentation for a long rectangular punch of width $2a$ versus $\beta = b/a > 1$, where b is a distance from the center of the punch at which the vertical displacement is imposed to be zero, $w(\pm b) = 0$. The normalizing indentation depth is $\delta_* = 2F/\pi E_*$, corresponding to a given value of F and $E_* = E/(1-\nu^2)$. For large values of β, the indentation depth is well approximated by $\delta/\delta_* = \ln(2\beta)$.

$$F = cE_*\delta\,, \quad c = \pi \frac{\int_0^1 p(\xi)\mathrm{d}\xi}{\int_0^1 p(\xi) \ln(\beta^2/\xi^2 - 1)\mathrm{d}\xi}\,, \quad \beta = \frac{b}{a}\,, \quad \xi = \frac{x}{a}\,. \tag{4.10}$$

If the contact pressure (per unit length of the punch) is assumed to be [7]

$$p(\xi) = \frac{p_0}{\sqrt{1-\xi^2}}\,, \quad p_0 = \frac{F}{\pi a}\,, \tag{4.11}$$

the substitution of (4.11) into (4.10) gives

$$c = \frac{\pi}{2\ln\left(\beta + \sqrt{\beta^2 - 1}\right)}\,, \quad F = \frac{\pi E_*}{2\ln\left(\beta + \sqrt{\beta^2 - 1}\right)}\,\delta\,. \tag{4.12}$$

The corresponding indentation stiffness $K_b = F/\delta = cE_*$ is

$$K_b = \frac{\pi E_*}{2\ln\left(\beta + \sqrt{\beta^2 - 1}\right)}\,, \tag{4.13}$$

where the subscript b is added to indicate that the stiffness depends on the choice of the value of b at which the vertical displacement is imposed to be zero, $w(x = \pm b) = 0$. For a given b, the indentation stiffness K_b is constant throughout the elastic indentation process, but it decreases with the increase of b. For example, $K_b = 1.1927E_*$ for $b = 2a$, while $K_b = 0.6852E_*$ for $b = 5a$. The plot of the normalized indentation depth δ as a function of $\beta = b/a$ is shown in Fig. 8. Geometrically, the normalizing depth $\delta_* = \delta(b = \beta_* a)$, where $\beta_* = (e + 1/e)/2 \approx 1.5431$. For large values of β (e.g., $\beta > 5$), the indentation stiffness is well approximated by $(\pi/2)E_*/\ln(2\beta)$. A recent study of the size effect in plane strain flat punch nanoindentation is reported in [34].

5 Conical indenter

Figure 9 shows a smooth rigid conical indenter with the cone angle α pressed into an isotropic elastic half-space with elastic properties (E, ν). The depth of the indentation due to applied force F is denoted by δ, the height of the conical cap in contact with the surrounding material is δ_0, and a is the corresponding radius of the contact. The conical contact in the (r, w) coordinate system is specified by

$$w(r) = \delta - r\cot\alpha\,, \quad r \leq a\,, \tag{5.1}$$

where $w(a) = \delta - \delta_0$ and $\delta_0 = a\cot\alpha$. A class of rigid indenters whose profile is of the type $\delta - w(r) = r^{2m}/(2R)^{2m-1}$ $(m > 1/2)$ were also considered for both elastic and inelastic indentation; for a spherical indenter $m = 1$, while for a conical indenter $m = 1/2$, with $(2R)^{2m-1}$ replaced with $\cot\alpha$ [35, 36]. Size effects in the conical indentation of an elasto-plastic solid were considered in [37], and elasto-plastic indentation of a hemispherical surface inclusion in [38].

5.1 Dimensional analysis

The relationship between F and δ is expected to involve the plane-strain modulus of elasticity $E_* = E/(1 - \nu^2)$ and the contact radius a. The cone angle α is included implicitly through the expected relationship between δ and a, because $a = \delta_0 \tan\alpha$, and by self-similarity of the conical indentation process it is expected that δ_0 is proportional to δ. Upon applying the Π theorem the following two independent non-dimensional groups can be identified

$$\Pi_1 = \frac{\delta}{a}\,, \quad \Pi_2 = \frac{F}{E_* a^2}\,, \tag{5.2}$$

which must be related in linear elasticity by

$$\frac{\delta}{a} = c_0\,\frac{F}{E_* a^2}\,, \quad c_0 = \text{const.} \tag{5.3}$$

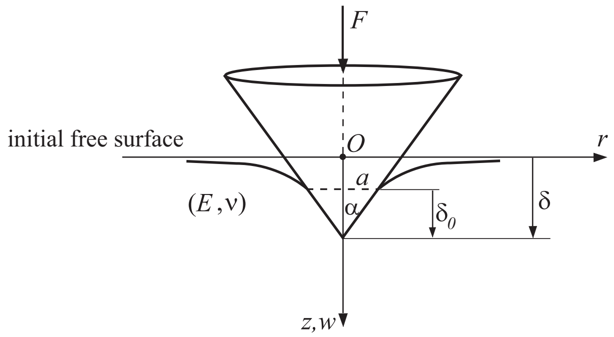

Figure 9: A conical indenter with the cone angle α pressed into an isotropic elastic half-space with elastic constants E and ν. The depth of the indentation due to the applied force F is δ. The height of the conical cap in contact with the material of a half-space is δ_0, and a is the corresponding radius of the contact.

Thus,

$$F = \frac{1}{c_0}\,\frac{E}{1-\nu^2}\,a\delta \equiv \frac{\tan\alpha}{c_0}\,\frac{E}{1-\nu^2}\,\delta_0\delta\,, \quad a = \delta_0\tan\alpha\,. \tag{5.4}$$

Furthermore, by self-similarity of conical indentation, we can write $\delta_0 = k\delta$, where $k = \text{const.}$, and (5.4) becomes

$$F = \zeta\tan\alpha\,\frac{E}{1-\nu^2}\,\delta^2\,, \quad \zeta = \frac{k}{c_0}\,, \tag{5.5}$$

which establishes the quadratic force-displacement relationship $F \sim \delta^2$.

Because F is proportional to δ^2, and a is proportional to δ_0 and thus δ ($a = k\delta\tan\alpha$), the average pressure in the contact region $\bar{p} = F/\pi a^2$ depends only on the cone angle α and the elastic constants, remaining unchanged throughout the indentation process,

$$\bar{p} = \frac{F}{\pi a^2} = \frac{1}{\pi c_0 k\tan\alpha}\,\frac{E}{1-\nu^2}\,. \tag{5.6}$$

5.2 Estimates of c_0 and k

By the same analysis as in section 2, see (2.8), if follows that the constant c_0 can be expressed in terms of the contact pressure as

$$c_0 = \frac{1}{\pi}\,\frac{\int_0^1 p(\rho)\mathrm{d}\rho}{\int_0^1 \rho p(\rho)\mathrm{d}\rho}\,, \quad \rho = \frac{r}{a}\,. \tag{5.7}$$

The constant k can also be expressed in terms of the contact pressure by imposing the condition that the work done by the force F on the displacement δ,

$$W_F = \int_0^\delta F(\delta)\mathrm{d}\delta = \frac{1}{3}\,F\delta\,, \quad F = \int_0^a p(r)2\pi r\mathrm{d}r\,, \tag{5.8}$$

must be equal to the work done by the contact pressure $p(r)$ on the displacement $w(r)$,

$$W_p = \frac{1}{2}\int_0^a p(r)w(r)2\pi r\mathrm{d}r\,, \quad w(r) = \delta - r\cot\alpha\,. \tag{5.9}$$

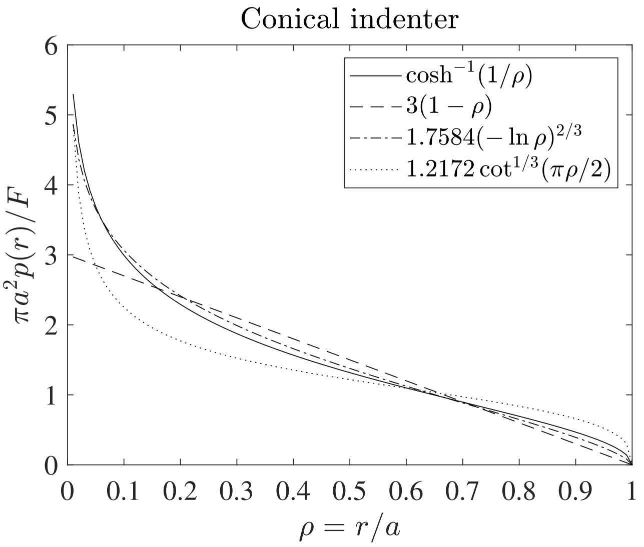

Figure 10: The shapes of four considered pressure distributions, normalized by the average pressure $\bar{p} = F/\pi a^2$, in the case of conical indentation. The coefficients shown in the figure legend are calculated so that the total force corresponding to each pressure distribution is equal to F.

It follows that

$$k = \frac{1}{3}\,\frac{\int_0^1 \rho p(\rho)\mathrm{d}\rho}{\int_0^1 \rho^2 p(\rho)\mathrm{d}\rho}. \tag{5.10}$$

To obtain the numerical values of c_0 and k, one needs to know or assume the pressure distribution $p = p(r)$ in the contact region $r \le a$. Because of the stress singularity at the apex of the cone, it is expected that $p(0)$ is singular (unbounded) at the center of the contact region $r = 0$. Furthermore, the pressure is expected to be zero along the contact edge $r = a$, with a steep (infinite) slope, similarly to the case of spherical indentation. Both of these features are embedded in the pressure distribution

$$p(r) = \bar{p}\cosh^{-1}(a/r)\,, \quad \bar{p} = \frac{F}{\pi a^2}\,, \tag{5.11}$$

where $\bar{p}$ is the average pressure. By substituting (5.11) into (5.7) and (5.10), if follows that

$$c_0 = 1\,, \quad k = \frac{2}{\pi}\,. \tag{5.12}$$

Consequently, $\zeta = 2/\pi$ in (5.5), and the force-displacement relationship becomes

$$F = \frac{2\tan\alpha}{\pi}\,\frac{E}{1-\nu^2}\,\delta^2\,, \tag{5.13}$$

while $\delta_0 = (2/\pi)\delta$. The average pressure (5.6) is

$$\bar{p} = \frac{F}{\pi a^2} = \frac{1}{2\tan\alpha}\,\frac{E}{1-\nu^2}\,. \tag{5.14}$$

The force-displacement relationship (5.13) is the correct relationship, because the assumed pressure distribution (5.11) is the actual pressure distribution obtained in the full elasticity solution of the conical indentation ([10], eq. (5.4.5), p. 96; [11], p. 190). The elastic indentation stiffness varies linearly with δ, i.e., $K = \partial^2 U/\partial\delta^2 = \partial F/\partial\delta = (4E_* \tan\alpha/\pi)\delta$, where $U = F\delta/3 = (4E_* \tan\alpha/3\pi)\delta^3$ is the strain energy stored in the half-space.

If the correct pressure distribution (5.11) was not recognized or known, and if instead the linear pressure distribution $p(r) = 3\bar{p}(1-\rho)$ was used in (5.7) and (5.10), the calculated coefficients would be $c_0 = 0.9549$ and $k = 0.6667$, giving $\zeta = k/c_0 = 0.6981$, which is less than 10% different from the correct value $\zeta = 0.6366$. The pressure distribution $p(r) = -2\bar{p}\ln\rho$ gives $\zeta = 0.589$, which is less than 7.5% smaller than the correct value. If a trial pressure distribution is $p(r) \sim \bar{p}[-\ln(\rho)]^{2/3}$, then $c_0 = 1.0106$, $k = 0.6552$, and $\zeta = 0.6483$, which is less than 2% greater than the correct value of 0.6366. The pressure distribution $p(r) \sim \bar{p}\cot^{1/3}(\pi\rho/2)$ also gives an error of only 2% ($\zeta = 0.6496$). The plots of the four considered pressure distributions are shown in Fig. 10.

6 Conclusion

The force-displacement relationships for indentation of isotropic elastic half-space by a rigid spherical ball, circular cylinder, circular cone, and flat cylindrical or rectangular punches are derived up to a single constant by dimensional analysis and by simple geometric and mechanics considerations, which include referrals to the Boussinesq and Flamant problems only, without solving the entire indentation boundary value problem at hand. To specify the unknown constant, the expression for the contact pressure distribution needs to be reasonably assumed. If this is the correct pressure distribution, e.g., a semi-ellipsoidal (semi-elliptical) in the case of spherical (cylindrical) indentation, the exact value of the constant is obtained, but using any reasonable trial pressure distribution, including a uniform pressure distribution in the case of indentation by a spherical ball, gives an error of less than 5%. For conical indentation, the use of the inverse cosine hyperbolic pressure distribution gives the exact value of the coefficient, but using even a linear pressure distribution gives an error of less than 10%. The results obtained for other approximate pressure distributions are discussed. The indentation stiffness is evaluated for all considered types of indentation. From the experimental point of view, because for each considered indenter only one parameter in the force-displacement relationship is not specified by the presented analysis exactly, only one data point is needed to fully specify the force-indentation relationship, without making any assumption about the contact pressure.

References

[1] Tabor, D., Hardness of Metals, Clarendon Press, Oxford, 1951.

[2] Oliver, W.C., Pharr, G.M., An improved technique for determining hardness and elastic modulus using load and displacement sensing indentation experiments, J. Mater. Res., Vol. 7, 1564–1583, 1992. https://doi.org/10.1557/JMR.1992.1564

[3] Bower, A.F., Fleck, N.A., Needleman, A., Ogbonna, N., Indentation of a power law creeping solid, Proc. R. Soc. Lond. A, Vol. 441, 97–124, 1993. https://doi.org/10.1098/rspa.1993.0050

[4] Oliver, W.C., Pharr, G.M., Measurement of hardness and elastic modulus by instrumented indentation: Advances in understanding and refinements to methodology, J. Mater. Res., Vol. 19, 1–20, 2004. https://doi.org/10.1557/jmr.2004.19.1.3

[5] Callister, Jr., W.D., Materials Science and Engineering: An Introduction, 10th ed., John Wiley, New York, 2019.

[6] Smith, W.F., Hashem, J., Prakash, R., Materials Science and Engineering, 5th ed., McGraw-Hill, New York, 2010.

[7] Johnson, K.L., Contact Mechanics, Cambridge Univ. Press, Cambridge, 1985.

[8] Gladwell, G.M.L., Contact Problems in the Classical Theory of Elasticity, Springer Science & Business Media, Dordrecht, 1980.

[9] Barber, J.R., Contact Mechanics, Springer Internat. Publ., Cham, 2018. https://doi.org/10.1007/978-3-319-70939-0

[10] Fischer-Cripps, A.C., Introduction to Contact Mechanics, 2nd ed., Springer Science & Business Media, New York, 2007.

[11] Sackfield, A., Hills, D.A., Nowell, D., Mechanics of Elastic Contacts, Butterworth-Heinemann, Oxford, 2013. https://doi.org/10.1016/C2009-0-24029-3

[12] Taylor, E.S., Dimensional Analysis for Engineers, Clarendon Press, Oxford, 1974.

[13] Barenblatt, G.I., Dimensional Analysis, CRC Press, Boca Raton, 1987.

[14] Borodich, F.M., Similarity methods in Hertz contact problems and their relations with Meyer hardness test, Techn. Report TR/MAT/FMB/98-98, Department of Mathematics, Glasgow Caledonian University, Glasgow, pp. 1–45, 1998. https://doi.org/10.13140/RG.2.1.3918.2167

[15] Cheng, Y.-T., Cheng, C.-M., Scaling, dimensional analysis, and indentation measurements, Mater. Sci. Eng. R, Vol. 44, 91–149, 2004. https://doi.org/10.1016/j.mser.2004.05.001

[16] Timoshenko, S.P., Goodier, J.N., Theory of Elasticity, 3rd ed., McGraw-Hill, New York, 1970.

[17] Hill, R., Störakers, B., A concise treatment of axisymmetric indentation in elasticity, in Elasticity: Mathematical Methods and Applications (G. Eason & R.W. Ogden, eds.), Ellis Horwood Ltd, pp. 199–209, 1990.

[18] Lubarda, M.V., Lubarda, V.A., Intermediate Solid Mechanics, Cambridge Univ. Press, Cambridge, 2020.

[19] Popov, V.L., Contact Mechanics and Friction. Physical Principles and Applications, Springer-Verlag, Berlin, 2010. https://doi.org/10.1007/978-3-642-10803-7

[20] Hill, R., Störakers, B., Zdunek, A.B., A theoretical study of the Brinell hardness test, Proc. R. Soc. Land. A, Vol. 423, 301–330, 1989. https://doi.org/10.1098/rspa.1989.0056

[21] Ghaednia, H., Wang, X., Saha, S., Xu, Y., Sharma, A., Jackson, R.L., A review of elastic-plastic contact mechanics. Appl. Mech. Reviews, Vol. 69, 060804-1–30, 2017. https://doi.org/10.1115/1.4038187

[22] Lubarda, V.A., Lubarda, M.V., On the depth of cylindrical indentation for two types of displacement constraints, arXiv:2309.02361 [physics.app-ph], 2023.

[23] Norden, B.N., On the compression of a cylinder in contact with a plane surface, National Bureau of Standards, Washington DC, 1973. https://www.nist.gov/system/files/documents/calibrations/nbsir_73-243.pdf

[24] Li, Q., Popov, V.L., Normal line contact of finite-length cylinders, Facta Universitatis, Series Mech. Eng., Vol. 15, 63–71, 2017. https://doi.org/10.22190/FUME170222003L

[25] Li, M., Zhang, H.-X., Zhao, Z.-L., Feng, X.-Q., Surface effects on cylindrical indentation of a soft layer on a rigid substrate, Acta Mech. Sinica, Vol. 36, 422–429, 2020. https://doi.org/10.1007/s10409-020-00941-8

[26] Meijers, P., The contact problem of a rigid cylinder on an elastic layer, Appl. Sci. Res., Vol. 18, 353–383, 1968. https://doi.org/10.1007/BF00382359

[27] Greenwood, J.A., Barber, J.R., Indentation of an elastic layer by a rigid cylinder, Int. J. Solids Struct., Vol. 49, 2962–2977, 2012. https://dx.doi.org/10.1016/j.ijsolstr.2012.05.036

[28] Long, J.M., Yuan, W., Chen, W., Wang, G.F., Analytic relations for two-dimensional indentations with surface tension, Mech. Mater., Vol. 119,34–41, 2018. https://doi.org/10.1016/j.mechmat.2018.01.003

[29] Jia, N., Yao, Y., Yang, Y., Chen, S., Analysis of two-dimensional contact problems considering surface effect, Int. J. Solids Struct., Vol. 125, 172–183, 2017. https://doi.org/10.1016/j.ijsolstr.2017.07.007

[30] Yuan, W., Wang, G., Cylindrical indentation of an elastic bonded layer with surface tension, Appl. Math. Model., Vol. 65, 597–613, 2018. https://doi.org/10.1016/j.apm.2018.09.001

[31] Giannakopoulos, A.E., Pallot, P., Two-dimensional contact analysis of elastic graded materials, J. Mech. Phys. Solids, Vol. 48, 1597–1631, 2000. https://doi.org/10.1016/S0022-5096(99)00068-X

[32] Vasu, T.S., Bhandakkar, T.K., Plane strain cylindrical indentation of functionally graded half-plane with exponentially varying shear modulus in the presence of residual surface tension, Int. J. Mech. Sci., Vol. 135, 158–167, 2018. https://doi.org/10.1016/j.ijmecsci.2017.11.009

[33] Zisis, Th., Gourgiotis, P.S., Cylindrical indentation in micropolar elasticity. Appl. Math. Model., Vol. 104, 373–385, 2002. https://doi.org/10.1016/j.apm.2021.11.033

[34] Campbell, C.J, Gill, S.P.A., An analytical model for the flat punch indentation size effect. Int. J. Solids Struct., Vol. 171, 81–91, 2019. https://doi.org/10.1016/j.ijsolstr.2019.05.004

[35] Hill, R., Similarity analysis of creep indentation tests, Proc. R. Soc. Lond. A, Vol. 436, 617–630, 1992. https://doi.org/10.1098/rspa.1992.0038

[36] Sneddon, I.N., The relation between load and penetration in the axisymmetric Boussinesq problem for a punch of arbitrary profile, Int. J. Eng. Sci., Vol. 3, 47–57, 1965. https://doi.org/10.1016/0020-7225(65)90019-4

[37] Danas, K., Deshpande, V.S., Fleck, N., Size effects in the conical indentation of an elasto-plastic solid, J. Mech. Phys. Solids, Vol. 60, 1605–1625, 2012. https://doi.org/10.1016/j.jmps.2012.05.002

[38] Eumelen, G.J.A.M., Suiker, A.S.J., Bosco. E., Fleck, N.A., Analytical model for elasto-plastic indentation of a hemispherical surface inclusion, Int. J. Mech. Sci., Vol. 224, 107267, 2022. https://doi.org/10.1016/j.ijmecsci.2022.107267

Uspostavljanje veze između sile i dubine indentacije bez potpunog rješavanja problema granične vrijednosti

Sažetak

Veza između sile i dubine indentacije u slučajevima sferne, cilindrične i konične indentacije je uspostavljena bez potpunog rješavanja korespondentnog problema granične vrijednosti, s preciznošću do jedne konstante. Ovo je postignuto korišćenjem dimenzionalne analize, u sprezi s elementarnom geometrijskom i mehaničkom analizom problema koncentrisane sile koja djeluje na površini dvodimenzionog ili trodimenzionog poluprostora. Da bi se odredila nepoznata konstanta, dovoljan je samo jedan experimentalni podatak o vezi sile i dubine elastične indentacije, i bez poznavanja rasporeda pritiska u zoni kontakta. Ukoliko je raspored pritiska precizno ili približno određen, vrijednost konstante slijedi analitičkim putem. Rezultati dobijeni korišćenjem tačne i približne raspodjele pritiska u zoni kontakta su upoređeni i diskutovani za sve razmatrane vrste indentacije.

Ključne riječi: cilindrični indenter; dimenzionalna analiza; indentacija; konični indenter; kontakt mehanika; pritisak; sferni indenter